Journal of Power Sources 208 (2012) 397–403

Contents lists available at SciVerse ScienceDirect

Journal of Power Sources

journal homepage: www.elsevier.com/locate/jpowsour

Niobized AISI 304 stainless steel bipolar plate for proton exchange membrane fuel cell

Lixia Wang, Juncai Sun*, Pengbin Li, Bo Jing, Song Li, Zhongsheng Wen, Shijun Ji

Institute of Materials and Technology, Dalian Maritime University, Dalian 116026, China

ARTICLE INFO

Article history:
Received 10 December 2011
Received in revised form 17 February 2012
Accepted 20 February 2012
Available online 1 March 2012

Keywords:
Proton exchange membrane fuel cell
Bipolar plates
Niobizing
Interfacial contact resistance
AISI 304 stainless steel
Corrosion resistance

ABSTRACT

AISI 304 stainless steel (SS) has been niobized by a plasma surface diffusion alloying method. A 3 μm niobized layer with dominant niobium elements has been formed on the 304 SS surface and the performances of the niobized 304 SS has been examined and evaluated as bipolar plate for proton exchange membrane fuel cell (PEMFC). Results show that the average contact angle with water for the niobized 304 SS is about 90.4°, demonstrating better hydrophobicity as compared with the untreated 304 SS (68.1°). The corrosion resistance of the 304 SS is considerably improved by the niobized layer with the corrosion current densities decreased at 0.2 and 0.4 μA cm^{-2} in simulated PEMFC anode purged with hydrogen and the cathode purged with air condition (0.05 M H_2SO_4 + 2 ppm F^- solution at 70 °C), respectively. The interfacial contact resistance (ICR) for the as-prepared niobized 304 SS is 10.53 mΩ cm^2 at the compaction of 140 N cm^{-2}. Furthermore, after 4 h potentiostatic tests, the niobizied specimens exhibit much lower ICR than that for the untreated ones. Thus, the niobized layer can act as a conductively protective layer of the 304 SS bipolar plate for PEMFC.

© 2012 Elsevier B.V. All rights reserved.

1. Introduction

Fuel cell is a cleaner, quieter and more efficient energy conversion device in comparison with the internal combustion engines. Among the many developed fuel cells, proton exchange membrane fuel cell (PEMFC), using hydrogen as a fuel, is expected to become a major power source for electrical vehicles and portable applications because of the following merits: high efficiency, operating at low temperature (<100 °C), faster startups at room temperature, environment friendliness, noiselessness, etc. [1–3]. Bipolar plate, which accounts for the dominant share of the total stack weight and cost, is a significant multifunctional component of the PEMFC stack [4]. The bipolar plate is designed to distribute fuel and oxygen, collect current, connect electrically the anode of one single cell to the cathode of adjacent single cell, prevent leakage of reactants and coolant as well as facilitate water and heat management. The PEMFC operating environments contain ions such as F^-, SO_4^{2-}, SO_3^{2-}, HSO_4^-, HSO_3^-, CO_3^{2-}, HCO_3^-, and a voltage difference between cathode and anode is up to 1 V while starting the PEMFC system [5]. Therefore, the bipolar plate needs to possess excellent electrochemical corrosion resistance as well as to have high bulk and contact electrical conductivity. Besides, relatively low cost, high strength, small volume as well as good hydrophobicity are also required for the bipolar plate materials [6,7].

Efforts are underway to develop bipolar plate materials that satisfy these demands. In the past decade, metallic bipolar plate, particularly stainless steels (SS), has been drawn much attention [8], due to their low cost, good physical and mechanical properties, mass production via stamping or embossing of sheet product, very thin form (<150 μm) [9,10]. However, the operating conditions of PEMFC are so harsh acidic and humid that the bare stainless steels cannot be successfully applied into a commercial PEMFC stack in terms of corrosion resistance. The metal ions produced by the corrosion dissolution of the stainless steel will further contaminate the electrode catalyst and result in the reduction of the cell performance. Besides, passive film formed on the surface of stainless steel under the PEMFC stack operation condition will decrease the interfacial contact resistance (ICR) and accordingly reduce the power output of the fuel cell [11]. Therefore, various surface modification techniques and methods on stainless steels have been applied to improve the corrosion resistance and the interfacial contact resistance simultaneously. Transition metals and their nitrides (e.g. CrN [12], TiN [13,14], etc.), carbides (e.g. Cr–C [15,16], TiC [17], etc.) as well as multilayer (e.g. Cr/CrN/Cr [18], Ti/TiN, Ti/CrN [19], etc.) have been widely fabricated as the protective layers for stainless steel bipolar plate and evaluated in simulated PEMFC conditions. As to the physical, chemical and electrical deposition coatings stated above, the challenges lie in eliminating and avoiding the inherent microcrack, micropore or pinhole defects existed in coatings.

* Corresponding author. Tel.: +86 411 84727959; fax: +86 411 84727959.
E-mail address: sunjc@dlmu.edu.cn (J.C. Sun).

0378-7753/$ – see front matter © 2012 Elsevier B.V. All rights reserved.
doi:10.1016/j.jpowsour.2012.02.075

Wang et al. [10] adopted a Cr-electroplating plus high temperature diffusion method to form a high Cr layer. Nam and Lee [20] have nitrided the Cr-electroplating coating to form a Cr_2N layer. Feng et al. [21] have applied a Ni—Cr co-ion implantation on 316L stainless steel to get a surface modified layer. Although a dense surface modified layer is obtained, the performances in corrosive resistance and surface electrical conductivity are still not satisfactory. Braindy et al. [22] have fabricated a dense CrN layer by thermal gas (N_2) nitridation of Ni50Cr50 alloy with good corrosion resistance and surface conductivity, but the cost of Ni50Cr50 alloy is not accepted by commercial application.

Niobium is widely used as a micro-alloying element in steel by means of solid solution formation, precipitation, carbide and coherent phase formation. Also, niobium and its alloys have excellent resistance to a wide variety of corrosive environment including mineral acids and most organic acids [23]. Report has disclosed the rate of niobium metal loss of <0.2 μm yr^{-1} in boiling 1 M H_2SO_4 solution [24]. Weil et al. [25] fabricated a niobium external cladding layer (50 μm thick) on 430 SS sheet by roll cladding method. As with the monolithic niobium, the Nb/430 SS shows high conductivity as well as perfect corrosion resistance. Nonetheless, the cost of the thick Nb cladding layer is expensive and the thickness reduction of Nb cladding layer is difficult in roll cladding. Pozio et al. [26] have also evaluated the niobium-coated 430 SS (SS430/Nb) with a 5 μm niobium clad layer and obtained promising results in terms of low corrosion current density and ICR value, which are in accordance with those acquired from Weil et al. [25]. However, an optimal thickness for the SS430/Nb specimens should be found to avoid internal corrosion of SS430 due to the penetration of corrosive media. Feng et al. [27] reported a niobium implantation method on SS316L. It is proved that the niobium implanting with proper ion fluencies can significantly improve the corrosion resistance of SS316L in the simulated PEMFC environment. However, the improved ICR for the niobium implanted SS316L seems still too high to be available for PEMFC bipolar plate, although the ICR value is lower than that for the bare SS316L.

In our previous work [28], a niobium nitride diffusion coating had been prepared on the surface of AISI 304 SS (Nb–N 304 SS) by plasma diffusion alloying method, meanwhile, the electrochemical and conductive properties of the specific coating were obtained. Those results demonstrate that the niobium nitride diffusion coating as a protective layer for 304 SS bipolar plate is electrochemically viable, i.e. considerably improving corrosion resistance as well as greatly decreasing ICR in simulated PEMFC operating condition. In that work, the preparation of the niobium nitride diffusion layer adopted a process of two consequent steps, which contained the niobium diffusion alloying (first step) followed by a niobium nitride formation and diffusion (second step) [28]. In this study, a thin niobium-alloyed (niobized) layer has been fabricated on the surface of 304 SS by simply one step: the niobium diffusion alloying process (niobizing) in a relative short time. The characteristics of the thin niobized layer to be used as a protective layer of 304 SS have been examined and evaluated under the simulated PEMFC operating conditions.

2. Experimental

2.1. Specimen preparation

AISI 304 SS sheets (thickness 1.5 mm) were cut into specimens of 10 mm × 10 mm as substrate materials in this study. Specimens were ground respectively with #360, #500, #800, #1000, #1500 grit SiC abrasive papers, polished mechanically with diamond paste, rinsed with acetone in an ultrasonic cleaner and lastly dried at room temperature.

The niobized layer was formed on the surface of 304 SS in a double glow plasma alloying furnace, which has three electrodes: an anode, a negative cathode (specimens) and a sputtering source cathode (Nb sinter plate). The specimens as a cathode were firstly heated and sputtering cleaned at 1173 K by work power supply and pure argon ion bombardment in the chamber at the pressure of 40 Pa and voltage of −1 kV. By keeping specimens at 1173 K, then, the source electrode power supply was loaded and kept at −800 to −900 V, meanwhile the working voltage of specimens was decreased to −530 to −580 V, which can allow more alloy sputtering elements to move from the source electrode into the surface of specimens. Specimens were treated at 1173 K for 2 h as a niobium diffusion process, which is similar to the step one described in our previous preparation of the niobium nitride diffusion coating [28]. After plasma surface niobium diffusion alloying processing (i.e. niobizing), scanning electron microscopy (SEM, Philip XL-40) in combination with energy-dispersive X-ray analysis Spectrometer (EDS, EDAX Instrument) was used to observe and analyze the niobized layer. The EDS was carried out in round 50 nm beam diameter at 15 kV acceleration voltage. In addition, the surface contact angle with water was also measured by a contact angle system SL200B.

2.2. Interfacial contact resistance measurements

ICR under various compaction forces were measured following the method described in Ref. [29]. The specimen was sandwiched between two carbon papers (Toray, Inc.) and the carbon paper/specimen/carbon paper sandwich was further put into two copper plates for force loading. In order to reduce the thermal effect of the current, a constant current (100 mA) provided by an YJ-10A type galvanostat was used via two copper plates. Changeable compaction forces were obtained through screwing a screw nut and a lead screw whose records were kept by a MCK-C compaction sensor, a special force gauge. Simultaneously, the variable potentials were recorded by a Solartron 7081 digital voltmeter with a precision of 10^{-8} V.

2.3. Electrochemical measurements

Potentiodynamic and potentiostatic tests were performed to measure the corrosion resistance of the bare and niobized specimens, respectively. A sulfuric acid solution (0.05 M H_2SO_4 + 2 ppm F^- solution) at 70 °C was used as an electrolyte in order to simulate the aggressive PEMFC environment [5–8]. The temperature of the corrosion test was maintained by an isothermal bath during electrochemical tests. Prior to each test, specimens were cleaned with ethanol then embedded in corrosion test cells. The corrosion test cell is constructed with PTFE material to fix and seal specimen as well as ensure only one side of the specimen contacting with the test solution for electrochemical measurements. The electrochemical measurements were conducted in a CHI660C electrochemical workstation controlled by a computer. A typical three-electrode system was used for the electrochemical measurements, in which a platinum sheet acted as the counter electrode, a saturated calomel electrode (SCE) connected to a Luggin capillary as the reference electrode and the specimens as the working electrode. All the specimens were stabilized at open circuit potential for 30 min before the electrochemical test, and then started the potential sweep from a specific voltage, a 0.2 V shift below the open circuit voltage, at a scanning rate of 1 mV s^{-1}. When potentiostatic tests were performed the −0.1 V (vs. SCE) potential with H_2 purging was applied to simulate the anodic environment and the 0.6 V (vs. SCE) potential with air purging was applied to simulate the cathodic environment [30].

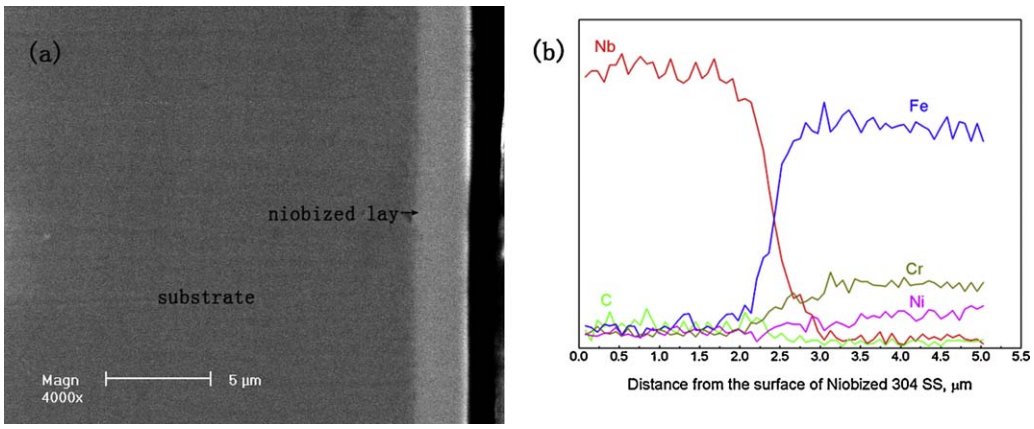

Fig. 1. (a) SEM micrographs of cross-section for niobized 304 SS. (b) Elemental EDS analysis for niobized layer.

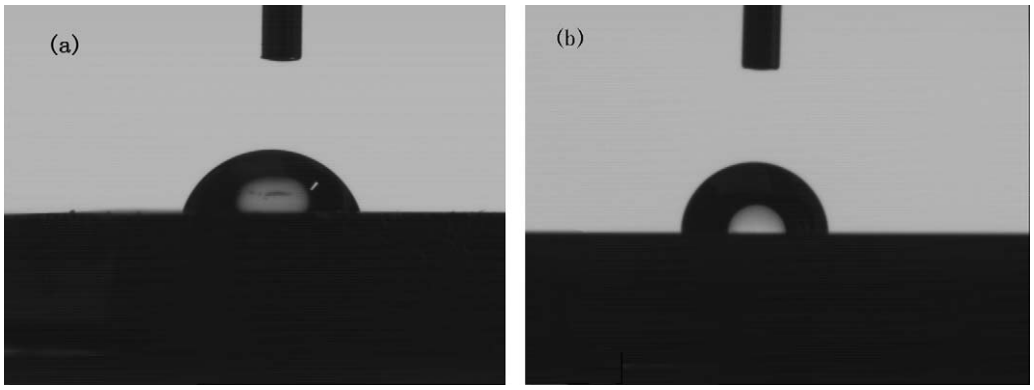

Fig. 2. Contact angle of the specimens with water: (a) untreated 304 SS and (b) niobized 304 SS.

3. Results and discussion

3.1. Characteristics of the niobized layer

Fig. 1(a) presents the cross-sectional view of the niobized 304 SS, it can be clearly seen that the thickness of the niobized layer is about 3 μm with uniform and dense microstructures. Also, the niobized layer displays well metallurgical adhesion to the substrate, which is free of defects such as pinhole, micropore and microcracks. EDS linear scanning curves of niobium, carbon, iron, chromium and nickel across the niobized layer are shown in Fig. 1(b). According to the variation of the above elements with different depth from the surface of niobized 304 SS, it can be again deduced that the niobized layer is about 3 μm, which is consistent with the result of micrograph. Obviously, Nb is the dominant element of the niobized layer. During the plasma diffusion alloying processing, Nb atoms was sputtered out from the source electrode and absorbed on the surface of the substrate owing to the bombardment of the argon ions and meanwhile diffused and penetrated into the substrate at high temperature. In addition, the carbon contained in the niobized layer is evidently more than that of the substrate bulk because of the strong chemical affinity with carbon of niobium.

In niobium rolling cladding method, Pozio et al. [26] suggested that the thickness of the niobium clad layer need to be more than 5 μm in order to prevent the penetration of corrosive media due to the inherent defects of the roll cladding method. However, the niobized layer in this study is metallurgically combined with the substrate. A very dense and thin niobized layer (~3 μm) without surface and interfacial defects is evidently beneficial to the surface protection of 304 SS bipolar plate.

3.2. Contact angle

In the PEMFC stack, the inlet gases need to be humidified to prevent the proton exchange membrane from dehydration. In addition, water would be generated owing to electrochemical reaction of the hydrogen and oxygen and meanwhile the exhausts are often mixed with the resultant water. Generally, the product water is expected in gas state and the flooding liquid water should be avoided in the PEMFC stack. Because the liquid water not only blocks the reaction gases accessing to the electrode, but also accelerates the corrosion of the metallic bipolar plates. Therefore, the redundant water must be removed from PEMFC stack in time. Hence, the materials of bipolar plate with good hydrophobicity would be helpful for water removal from the stack and beneficial to the simplification of water management. The feature of hydrophobicity is identified by contact angle with water. Four measurements are collected and calculated for each specimen to achieve an accurate average value. Fig. 2(a) and (b) shows the contact angle images of the untreated and niobized 304 SS with water, respectively. Table 1 displays all the calculated values. Apparently, the niobized 304 SS has a much bigger average contact angle with water (about 90.4°) than that of untreated 304 SS with value of 68.1°. Usually, a hydrophobic material displays a contact angle more than 90° between liquid–vapor

Table 1
Average contact angles with water of the specimens.

Specimens	Average contact angle (°)
Untreated 304 SS	68.1
Niobized 304 SS	90.4

Table 2
Corrosion current density and potential of specimens polarized in simulated PEMFC conditions.

Specimen	Purged with H_2		Purged with air	
	I_{corr} ($\mu A\,cm^{-2}$)	E_{corr} ($mV_{vs.SCE}$)	I_{corr} ($\mu A\,cm^{-2}$)	E_{corr} ($mV_{vs.SCE}$)
Untreated 304 SS	21.204	−347	13.453	−319
Niobized 304 SS	0.384	−11	0.461	80
Nb–N 304 SS [28]	0.127	100	0.071	143

and liquid–solid surfaces as a water droplet is placed onto its surface [31]. Therefore, the 304 SS with a niobized layer is suitable for the bipolar plate use in terms of the hydrophobicity.

3.3. Interfacial contact resistance

High electrical conductivity is a key factor for a commercial PEMFC bipolar plate. The ICR between the as-prepared niobized 304 SS and the carbon paper was measured under variable compaction forces as shown in Fig. 3. ICR values of the untreated one are also given for comparison. It can be observed that ICRs decrease considerably at relatively low compaction force (20–100 N cm^{-2}) then slowly, almost do not change at high compaction force (120–250 N cm^{-2}). Over the entire applied compaction force range, the ICRs of niobized 304 SS are much lower than that of the untreated one at the same compaction force. In more details, at the compaction of 140 N cm^{-2}, ICR is about 10.53 mΩ cm^2 for the niobized 304 SS which is approximated to that (9.26 mΩ cm^2) for the Nb–N 304 SS [28] and is extremely lower than that (100.98 mΩ cm^2) for untreated 304 SS under the same compaction force. In addition, the magnitude of ICR for niobized 304 SS is quite comparable to that of niobium clad 430 SS obtained by Weil [25] and Pozio et al. [26].

3.4. Electrochemical polarization and stability

Dynamic polarization of the niobizied 304 SS in 0.05 M H_2SO_4 + 2 ppm F^- solution at 70 °C purged with H_2 or air are shown in Fig. 4(a) and (b), respectively. For comparison, polarization curves of untreated 304 SS polarized in the same environments are also plotted. Although all the studied specimens show passive behavior, there are differences existed for the nobized 304 SS. Firstly, the corrosion potential (E_{corr}) is shifted to higher values, i.e. from −347 mV to −11 mV in simulated anodic environment and from −319 mV to 80 mV in simulated cathodic environment. Secondly, the untreated 304 SS shows a typical polarization curve of passive metals in both H_2 and air purged circumstances with active, passive and transpassive regions while the niobized 304 SS is almost free of active–passive transitions. These phenomena indicate that the niobized 304 SS is more easily passivated under the PEMFC environment. The results obtained from the polarization curves by linear-polarization method are shown in Table 2. As a comparison, the results of the Nb–N 304 SS [28] were also listed in the Table 2. It can be clearly seen that the corrosion resistance in simulated both the anodic and the cathodic environment of the materials above were ranked in the following order: Nb–N 304 SS > niobized 304 SS > untreated 304 SS in terms of the corrosion current densities (I_{corr}). The niobized 304 SS shows relatively less but comparable corrosion resistance by contrast to the Nb–N 304 SS. Therefore, the I_{corr} of niobized 304 SS is reduced by nearly two orders of magnitude in comparison with untreated 304

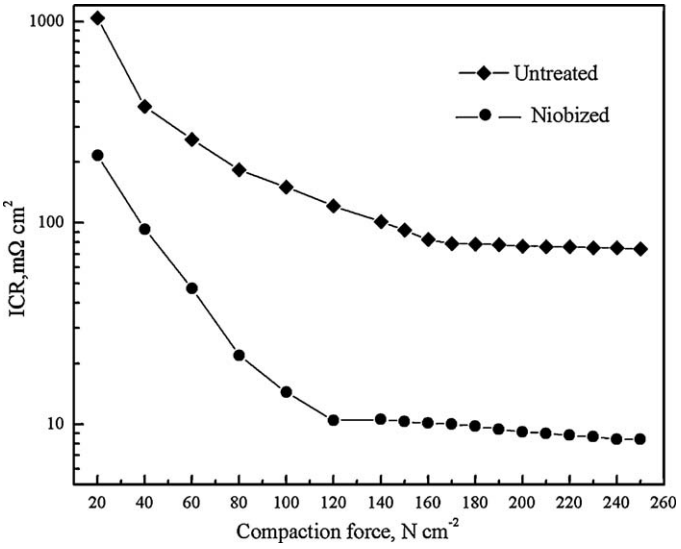

Fig. 3. ICR of untreated 304SS and niobized 304 SS under different compaction forces.

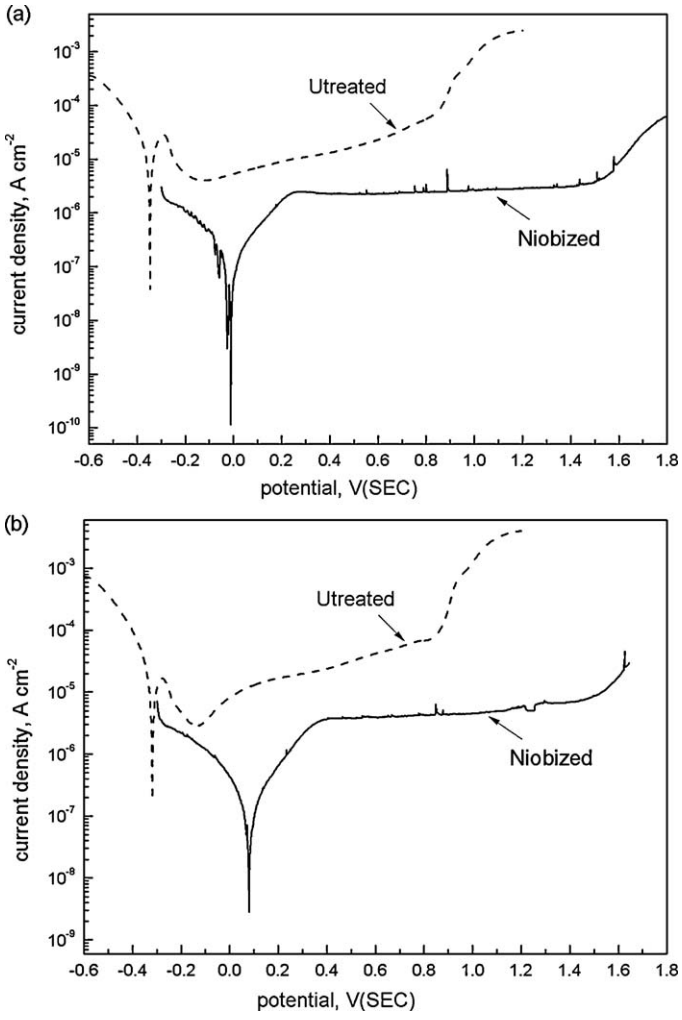

Fig. 4. Potentiodynamic polarization curves of untreated and niobized 304 SS in 0.05 M H_2SO_4 + 2 ppm F^- solution at 70 °C purged with H_2 (a) and air (b).

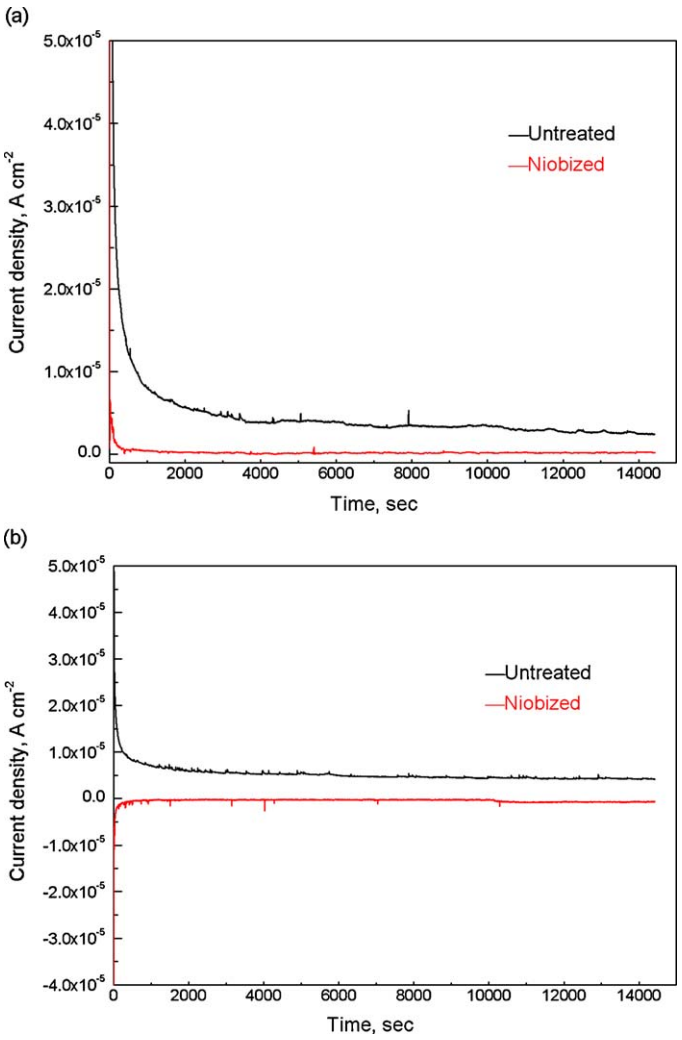

Fig. 5. Current density–time relationship of untreated and niobized 304 SS in 0.05 M H_2SO_4 + 2 ppm F^- solution at 70 °C purged with air (a) and H_2 (b).

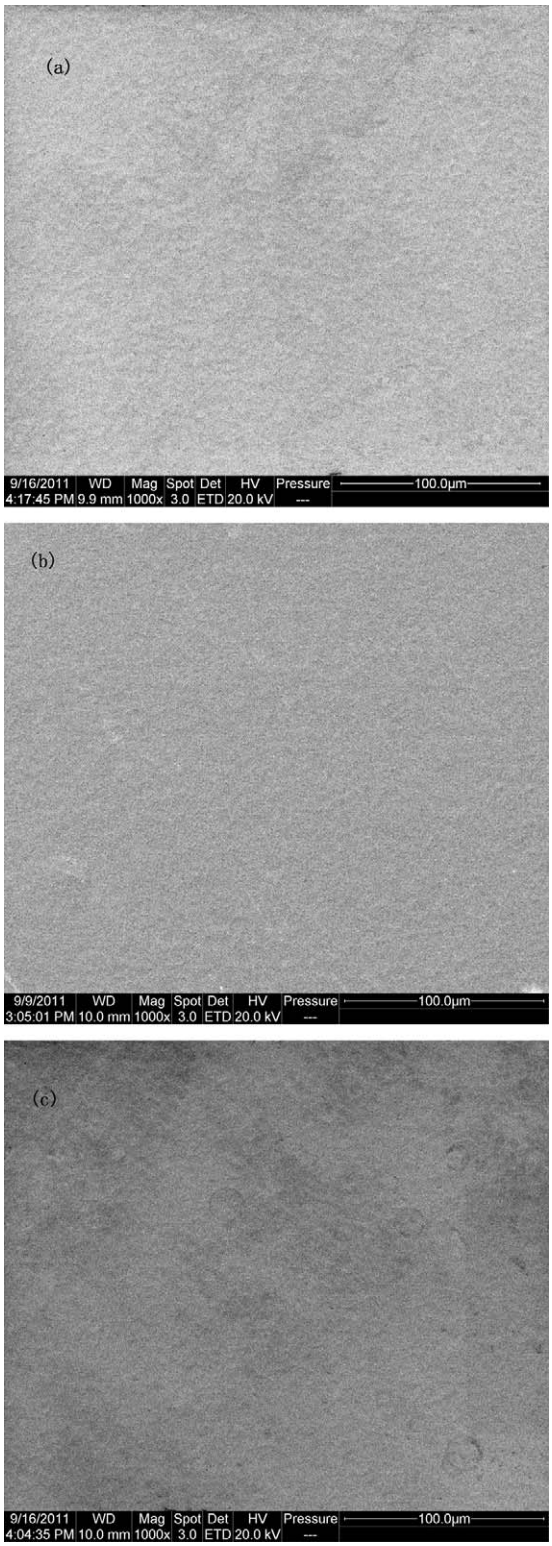

Fig. 6. SEM micrographs of niobized 304 SS (a) and after potentiostatic testing in simulated anodic (b) and cathodic (c) environment.

SS, demanstrating a great improvement in the corrosion resistance resulting from the niobized layer. Actually, the corrosion resistance of niobized 304 SS is fulfill the bipolar plate design target for corrosion rate <1 $\mu A\,cm^{-2}$ proposed by U.S. Department of Energy (DOE) [32,33].

Based on the promising potentiodynamic polarization results, potentiostatic tests were also performed to examine the stability of untreated and niobized 304 SS by monitoring the variation of current density as a function of time at cathode and anode in simulated PEMFC environment for a total time of 4 h. Fig. 5(a) displays the typical passivation behavior of the untreated and niobizied 304 SS under applied potential of 0.6 V_{SCE} with air purging. The current densities of all specimens diminish rapidly at the beginning but gradually stabilize at a quite low level, namely, about 7 $\mu A\,cm^{-2}$ and 0.4 $\mu A\,cm^{-2}$ for the untreated and niobized 304 SS, respectively. The quickly decay in current density of the untreated 304 SS is related to the formation of the passive film [34–37]. Once the whole surface is covered by passive film, the current density needed to maintain the passivation is quite low. In the anodic PEMFC environment purged with H_2, potentiostatic tests were carried out at −0.1 V as shown in Fig. 5(b). Likewise, all the test specimens show passivation in a short period of time, meanwhile the current densities stabilized at 10–5 $\mu A\,cm^{-2}$ and about −0.2 $\mu A\,cm^{-2}$ for the untreated and niobized 304 SS, respectively. Besides, the current density of the niobized 304 SS keeps negative during the entire test implying that the surface of niobized 304 SS is cathodically protected. Therefore, under this condition with cathodic (negative) current density there would be no more active dissolution of the niobium diffusion layer. According to the above results, all the test specimens show quite stable current densities, which demonstrate that the passive films are stable under both cathodic and anodic PEMFC environment. Meanwhile, the stable current

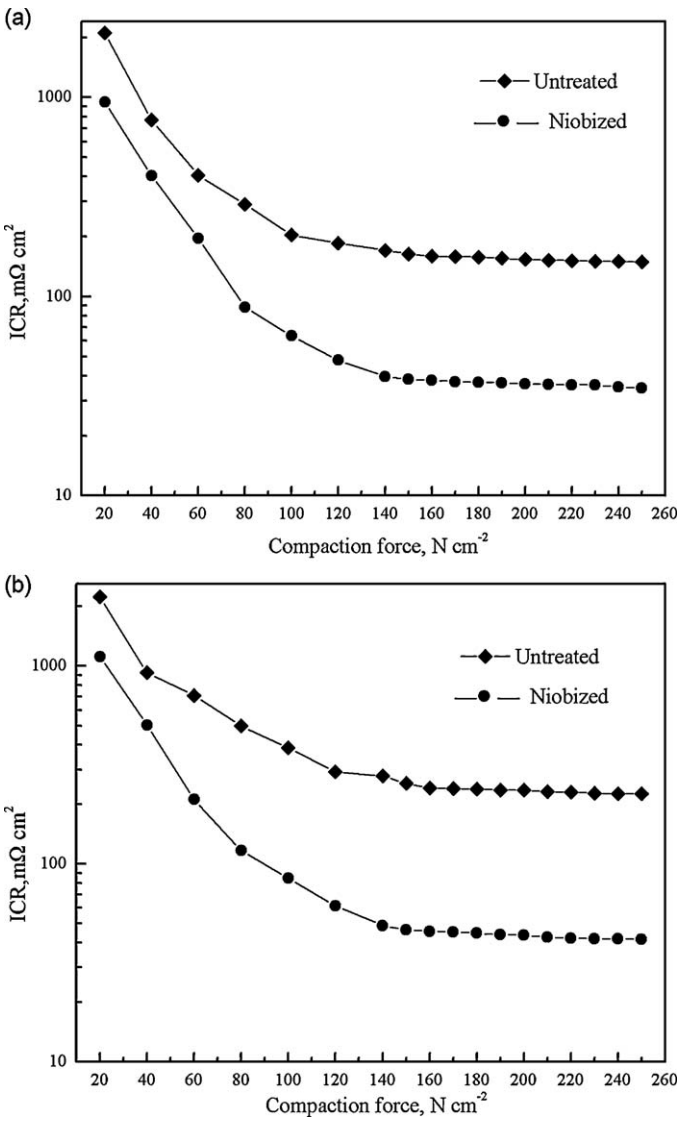

Fig. 7. ICR of untreated 304 SS and niobized 304 SS under different compaction forces after potentiostatic testing in simulated anodic (a) and cathodic (b) environment.

densities of niobized 304 SS are more than one order of magnitude lower than that of the untreated ones. Again, the 304 SS with niobium diffusion layer displays the improved anticorrosion behavior in the simulated PEMFC environment.

Fig. 6(a)–(c) presents comparisons of the surface morphologies examined by SEM of the niobized 304 SS before and after potentiostatic testing for 4 h in simulated anodic and cathodic environment, respectively. The initial surface morphology of niobizied 304 SS presented in Fig. 6(a) is dense, uniform and smooth without surface micropore, a common surface defect produced by the cladding method [25]. Fig. 6(b) and (c) shows virtually no difference in surface morphology compared with Fig. 6 (a), which can be verified the absence of corrosion at the surface of the niobized 304 SS after the potentiostatic test for 4 h in both the anodic and cathodic PEMFC environment.

As investigated by many researchers [33–35], in order to avoid further electrochemical corrosion, a passive film will be formed on the surface of stainless steel when the material is exposed to the aggressive acid and specific electrode potential operating condition of PEMFC. This passive film does prevent the substrate from further corrosion. However, it will increase the ICR because the main composition of the passive film formed on the surface of stainless steel in the PEMFC working conditions is semi-conductive Cr_2O_3. Therefore, the ICR of untreated and niobizd 304 SS after potentiostatic test in simulated anodic and cathodic environment were also measured under variable compaction force, as shown in Fig. 7(a) and (b). Apparently, referring to Fig. 3, ICRs of all the test specimens have increased at the same compaction force after potentiostatic polarization for 4 h in simulated PEMFC environment. However, the niobized 304 SS kept a relative stable ICR, while the untreated 304 SS showed obvious increase of ICR value, i.e. the increase of ICR for the niobized 304 SS is much smaller than that for the untreated specimens. In particular, at the compaction force of 140 N cm^{-2}, ICRs for niobized 304 SS are 39.61 mΩ cm^2 and 48.9 mΩ cm^2 after potentiostatic test in simulated anodic and cathodic environment, respectively. Considering the ICR (170.52 and 278.25 mΩ cm^2) for the untreated 304 SS after the similar corrosion test, these ICR values for the niobized 304 SS seem very low at the same compaction force, illustrating the beneficial effect of the niobized layer on the surface conductivity of the 304 SS. Furthermore, in the actual bipolar plate use with machined flow channels fabricated from the same materials, the measured ICR is lower at a nominal compaction force due to the smaller contact area than the simulated bipolar plate without flow channels [38]. Besides, Wang et al. [30] have pointed out that in a practical situation where water is produced in the PEMFC stack and the membrane is wet, the ICR should decrease in comparison with the ICR measured with dry specimens. Taken these views above into considerations, the niobized 304 SS presented in this work gives very promising ICR results.

4. Conclusions

Niobized 304 SS specimens were evaluated as the possible bipolar plate materials with respect to the hydrophobic property, surface conductivity as well as the corrosion resistance. The dense and uniform niobized layer has well metallurgical bonding with the substrate without facial and interfacial defects such as pinhole, micropore and microcracks. The much bigger contact angle with water suggests a better hydrophobic property of the niobized 304 SS, which is beneficial to the water management in the PEMFC stack and the anticorrosion of the bipolar plate itself. Surface conductivity measurements imply a considerable decrease of ICR for the niobized 304 SS due to the inherent high conductivity of the niobium and its alloys. Meanwhile, the corrosion resistance of the niobized 304 SS is considerably improved which is comparable to that of the niobium nitride modified 304 SS in terms of the corrosion current density and passivated behavior. Furthermore, after 4 h potentiostatic test in simulated PEMFC environment, surface conductivity of niobized 304 SS is prominently improved in contrast to the untreated specimens. Therefore, the niobized 304 SS shows greatly possibility to be used as the candidate bipolar plate for PEMFC.

Acknowledgement

This work is financially supported by the National Foundation of Natural Science of China under contract No. 21176034.

References

[1] N. Demirdoven, J. Deutch, Science 305 (2004) 974–976.
[2] M. Lefevre, E. Proietti, F. Jaouen, J.P. Dodelet, Science 324 (2009) 71–74.
[3] C.E. Borroni-Bird, J. Power Sources 61 (1996) 33–48.
[4] J. Wind, R. Spah, W. Kaiser, G. Bohm, J. Power Sources 105 (2002) 256–260.
[5] R.J. Tian, J.C. Sun, J. Power Sources 194 (2009) 981–984.
[6] A. Pozio, R.F. Silva, M.D. Francesco, L. Giorgi, Electrochim. Acta 48 (2003) 1543–1549.
[7] R.J. Tian, J.C. Sun, L. Wang, J. Power Sources 163 (2007) 719–724.
[8] R.J. Tian, J.C. Sun, J.L. Wang, Rare Metals 25 (October) (2006) 229, Spec. Issue.

[9] S.T. Hong, K.S. Weil, J. Power Sources 168 (2007) 408–417.
[10] J.L. Wang, J.C. Sun, S. Li, Z.S. Wen, S.J. Ji, Int. J. Hydrogen Energy 37 (2012) 1140–1144.
[11] R.J. Tian, J.C. Sun, L. Wang, Int. J. Hydrogen Energy 31 (2006) 1874–1878.
[12] Y. Fu, M. Hou, G. Lin, J. Hou, Z. Shao, B. Yi, J. Power Sources 176 (2008) 282–286.
[13] R.J. Tian, J.C. Sun, Int. J. Hydrogen Energy 36 (2011) 6788–6794.
[14] Y. Wang, D.O. Northwood, J. Power Sources 165 (2007) 293–298.
[15] Y. Fu, G. Lin, B. Wu, Z. Shao, B. Yi, Int. J. Hydrogen Energy 34 (2009) 6771–6777.
[16] S.B. Lee, K.H. Cho, W.G. Lee, H. Jang, J. Power Sources 187 (2009) 318–323.
[17] Y.J. Ren, C.L. Zeng, J. Power Sources 171 (2007) 778–782.
[18] M. Zhang, B. Wu, G. Lin, Z. Shao, M. Hou, B. Yi, J. Power Sources 196 (2011) 3249–3254.
[19] W.Y. Ho, H.J. Pan, C.L. Chang, J.J. Hwang, Surf. Coat. Technol. 202 (2007) 1297–1301.
[20] D.G. Nam, H.C. Lee, J. Power Sources 170 (2007) 268–274.
[21] K. Feng, Y. Shen, D. Liu, P.K. Chu, X. Cai, Int. J. Hydrogen Energy 35 (2010) 690–700.
[22] M.P. Brady, K. Weisbrod, I. Paulauskas, R.A. Buchanan, K.L. More, H. Wang, M. Wilson, F. Garzon, L.R. Walker, Scr. Mater. 50 (2004) 1017–1022.
[23] G.E. Cavigliasso, M.J. Esplandiu, V.A. Macagno, J. Appl. Electrochem. 28 (1998) 1213–1219.
[24] A. Robin, Int. J. Refract. Met. Hard Mater. 15 (1997) 317–323.
[25] K.S. Wei, G. Xia, Z.G. Yang, J.Y. Kim, Int. J. Hydrogen Energy 32 (2007) 3724–3733.
[26] A. Pozio, R.F. Silva, A. Masci, Int. J. Hydrogen Energy 33 (2008) 5697–5702.
[27] K. Feng, Z. Li, X. Cai, P.K. Chu, Surf. Coat. Technol. 205 (2010) 85–91.
[28] L.X. Wang, J.C. Sun, J. Sun, Y. Lv, S. Li, S.J. Ji, Z.S. Wen, J. Power Sources 199 (2012) 195–200.
[29] H. Wang, M.A. Sweikart, J.A. Turner, J. Power Sources 115 (2003) 243–251.
[30] R.L. Borup, N.E. Vanderborgh, Mater. Res. Soc. 393 (1995) 151.
[31] C.Y. Chung, S.K. Chen, T.S. Chin, T.H. Ko, S.W. Lin, W.M. Chang, S.N. Hsiao, J. Power Sources 186 (2009) 393–398.
[32] H. Tawfik, Y. Hung, D. Mahajan, J. Power Sources 163 (2007) 755–767.
[33] R.A. Antunes, M.C.L. Oliveira, G. Ett, V. Ett, Int. J. Hydrogen Energy 35 (2010) 3632–3647.
[34] K.E. Heusler, M. Schulze, Electrochim. Acta 20 (1975) 237–244.
[35] H. Wang, J.A. Turner, J. Power Sources 128 (2004) 193–200.
[36] T. Hurlen, H. Bentzen, S. Hornkjql, Electrochim. Acta 32 (1987) 1613–1617.
[37] M. Kumagai, S.T. Myung, S. Kuwat, R. Aasishi, H. Yashiro, Electrochim. Acta 53 (2008) 4205–4212.
[38] Y. Wang, D.O. Northwood, Adv. Mater. Res. 41/42 (2008) 469–475.